Joint Trajectory and Resource Allocation Design for Throughput Optimization in UANET

Tao Peng[1,2], Xiaoyang Li[1,2], Xiangyu Li[1,2], Rongrong Qian[3]

[1] Wireless Signal Processing and Network Laboratory, Beijing University of Posts and Telecommunications, China
[2] Key Laboratory of Universal Wireless Communication, Ministry of Education, China
[3] School of Artificial Intelligence, Beijing University of Posts and Telecommunications, China
pengtao@bupt.edu.cn , lixiaoyang111@bupt.edu.cn, lixymiracle@ bupt.edu.cn, rongrongqian@bupt.edu.cn

Abstract

Natural disasters and some emergencies may destroy the fixed communication infrastructures, and bring great inconvenience to information exchange among people. Unmanned aerial vehicles (UAVs) technology has attracted research interest and has made remarkable progress in recent years because of its great flexibility. In this paper, we propose a framework where UAVs act as temporary air base stations, and provide periodic internal communications for several user groups. We optimize their trajectories such that a weighted function of the minimal throughput is maximized. Firstly, we proposed a distributed gradient-based algorithm to find the optimal hovering positions for UAVs, which can improve the total throughput of each group. Then, we solved a mixed integer linear programming problem to determine the path of each available UAV. Through Shannon-Hartley Theorem, the system optimization objective is formulated by signal-to-noise ratio (SNR) that incorporates with UAV positions and ground user positions. UAVs will be arranged with reasonable paths and hovering time to increase the system throughput. Finally, simulation results verified the effectiveness of the proposed algorithm.

Keywords: UAV, Positioning, Path-planning, Throughput optimization

1 Introduction

With the maturity of Unmanned Aerial Vehicles (UAVs) technology and the increasing popularity of consumer UAVs, UAV applications in various fields have been developed rapidly. UAV has multiple interesting capabilities: wide range of coverage, low cost, easy deployment, and much less dependence of terrain. As mentioned in [1] and [2], it has a very broad application prospect in the field of wireless communication. With the increasing communication requirement in the wild, cluster intelligence and mobile ad hoc network (MANET) based on unmanned platforms has attracted wide interest and has become a new research hotspot in the field of wireless communication.

The UAV ad hoc network (UANET) is to apply the MANET technology to aerial platforms, so that the air platforms and the ground devices can form a no pre-existing, collaborative integrated, highly flexible self-organizing network. A number of advanced technologies related to this field, such as cloud computing and edge computing [3-4], Internet-of-Things (IoT) [5-6], forecast and recommendation system [7-8], explicitly demonstrate the importance of UANET.

Many valuable literatures have studied UANET and its optimization. In the related research area, quite a few communication metrics, such as coverage, connectivity, latency, energy efficiency and throughput, which are vital to reflect network performance, have been formulated and optimized.

For coverage, in [9], the optimal drone small cell (DSC) altitude, which leads to a maximum ground coverage and minimum required transmit power for a single DSC, was investigated. In the further work [10], circle packing theory was used to determine the 3-D locations of UAVs so that the total coverage area of a multiple UAVs wireless network could be maximized. [11] applied a multi-layout multi-subpopulation genetic algorithm to solve multi-objective coverage problems of UAV networks. It formulated a weighted fitness function considering relevant factors, and proved the superiority of new evolutionary concept.

With regard to connectivity, Z. Han et. al optimized the connectivity of MANET by smart deployment of UAV in [12]. They defined four types of network connectivity based on graph theory. According to their mathematical characteristics, a gradient-based algorithm was proposed and Delaunay triangulation (DT) was used to optimize the network connectivity.

The optimization of energy efficiency is also a hot topic, since most small UAVs are battery-powered and their energy is strictly limited. Efficient management is especially needed in their operation, where a significant portion of energy is consumed for flight and

*Corresponding Author: Tao Peng; E-mail: pengtao@bupt.edu.cn
DOI: 10.3966/160792642020112106020

hovering operations. [13] proposed a power model of drone's hover and transition. In [14], the problem of proactive deployment of cache-enabled UAVs for optimizing the quality-of-experience (QoE) of wireless devices in a cloud radio access network while minimizing the transmit power used by the UAVs is studied. To solve this problem, a novel algorithm based on the machine learning framework of conceptor-based echo state networks (ESNs) is proposed. In [15], the problem of dynamical deployment of UAVs equipped with visible light communication (VLC) capabilities for optimizing the energy efficiency of UAV-enabled networks is studied. An algorithm that combines the machine learning framework of gated recurrent units (GRUs) with convolutional neural networks (CNNs) is proposed. In [16], Q. Wu et. al studied a multi-UAV enabled wireless network where multiple UAVs serve as aerial base stations for a group of ground users. They proposed an algorithm based on block coordinate descent and successive convex optimization to jointly optimize the multiuser communication scheduling and association, UAV trajectory and transmit power control, so as to maximize the minimum throughput over all ground users in the downlink communication. [17] considered using UAV as mobile data collector in wireless sensor network to prolong the network lifetime. It jointly optimized the sensor nodes' wake-up schedule and UAV's trajectory to minimize the maximum energy consumption of all sensors by applying the successive convex optimization. A novel framework was proposed for the trajectory design of multiple UAVs in [18]. The problem of joint trajectory design and power control was formulated for maximizing the instantaneous sum transmission rate. To solve this pertinent problem, a three-step approach was proposed, which is based on machine learning techniques.

As for throughput, in [19] and [20], C. Dixon et al. proposed a distributed mobility control algorithm to optimize the end-to-end communication throughput of a UAV relay chain system. The chaining controller drives the real time location of UAVs, applying estimates of the communication objective function gradient calculated by stochastic approximation techniques, to improve the relay performance. In [21], Y. Sun et. al studied the joint design of the 3D aerial trajectory and the wireless resource allocation for maximization of the system sum throughput over a given time period. In particular, the UAV is powered by the solar energy enabling sustainable communication services to multiple ground users. [22] proposed a tractable method for drone base stations deployment based on the notion of truncated octahedron shapes which aims to minimize total latency. Zeng et. al [23] investigated the throughput maximization problem in a UAV relaying system by optimizing the source/relay transmit power along with the relay trajectory. [24] proposed an aerial-terrestrial cloud networks (ATCNs), global integration of air and ground communication systems which pave a way for a large set of applications such as surveillance, on-demand transmissions, data-acquisition, and navigation. In [25], a centralized heuristic algorithm was proposed for positioning UAVs to maximize the throughput of a software-defined disaster area UAV communication network. [26] considered an aerial base station assisted terrestrial network where user mobility is considered. To optimize the total throughput, an approach based on a discounted reward reinforcement learning, which is known as Q-learning, was proposed.

Although the objectives of above literatures are different, the means, by optimizing UAV deployment or trajectory design, are the same. The algorithms can be divided into five categories: heuristic algorithm [11, 25], gradient based search [12, 19-20], successive convex optimization [16-17, 23], geometric method [10, 12] and machine learning [18, 26-27]. Different algorithms are suitable for different problems in different network models. In this field of research, a practical network model is an important prerequisite.

In this paper, we propose a UANET model according to the communication demand in a search-and-rescue scenario. We jointly optimize the UAV deployment, relay trajectory and resources allocation for a multi-UAV enabled relay network to improve the network total end-to-end throughput. UAVs apply two strategies when providing service which aims to guarantee multi-groups' end-to-end communication requirements by their high mobility. Firstly, we propose a decentralized UAV positioning algorithm to optimize the total end-to-end throughput of each group. Compared with the mainstream heuristic iteration algorithm like Particle swarm optimization (PSO) [28], our algorithm can significantly reduce the complexity, and there is almost no difference in optimization performance. Then, the trajectories of UAVs aiming to cover different groups can be obtained after solving a mixed integer linear programming problem (MILP). We consider the decode-and-forward (DF) method as the end-to-end communication capacity model [29], and formulate the system optimization target by Shannon-Hartley Theorem based on the received signal-to-noise ratio (SNR). The stochastic approximation is utilized to estimate the generalized gradient, and the convergence of the objective function to local maximal is proved by using the non-smooth stability analysis literature [30]. The optimization effectiveness is validated by simulation results.

The remainder of this paper is organized as follows. Section II describes the system model. Section III proposes problem formulation. Section IV provides the detailed description of the proposed positioning algorithm and the design of relay trajectory and resource allocation. Section V shows the result of simulation experiments. In Section VI, we conclude this work.

2 System Model

After a natural disaster such as earthquake or flood, the fixed communication infrastructure may not be available in a large area. Searchers and rescuers usually form multiple independent groups in different places. There is no way for direct communication among group members who perform collaborative tasks in different regions. Due to the complex ground environment, vehicle base stations can't help a lot. In this case, it is attractive to use multiple UAVs as communication relay because of their mobility and large coverage. In this paper, we consider a dynamic UAV network which provides communication services for multiple groups.

2.1 System Model of UANET

As shown in Figure 1, independent user groups are performing different tasks in the large area at the same time, and users usually only require communication with other users in the same group. UAVs are arranged to provide relay services for all the groups by turns. Due to the limited number of UAVs, it is impossible to provide relay services for all the groups simultaneously. UAVs need to adopt a certain flight strategy to take care of different user groups on ground within a period of time T. In Figure 1 a single UAV serves a specific group (Group 4), and the UAV establishes communication links with all users in the service group. In Figure 2, the top view of Group 1 shows how multiple UAVs work when serving the same group, where each user establishes a link with one of the drones, and the two drones are connected through independent channels to relay the user data. For this model, we make the following assumptions:

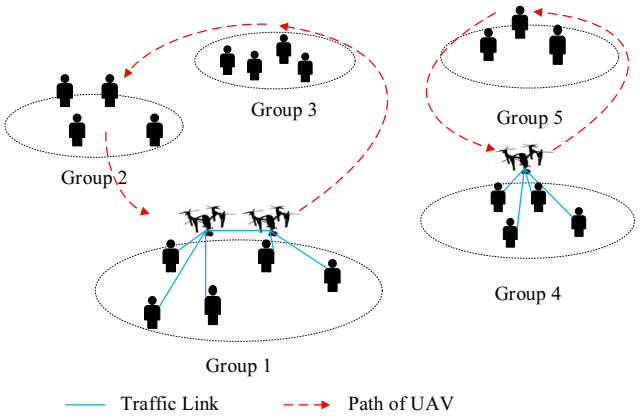

Figure 1. A sample system model of three UAVs serving five groups

- The users in a group cannot communicate directly with other users in the same group without relays. The UAV communication range can cover the active zone of a group, and UAVs can communicate with each other directly.
- Each user has incontinuous willingness to exchange messages with all other users in the same group, and the messages are time-insensitive which have a great tolerance for delay.
- Each UAV is equipped with multi-radios which occupy different orthogonal channels, while each ground user only has one. A user can only establish communication link with up to one UAV, so all the messages of this user need to pass through this drone.

Figure 2 shows the top view of Group 1 in Figure 1, where multiple UAVs serve one group. We define those users who are directly connected to the same UAV as this UAV's sub-network. Users in the same sub-network share a communication channel by time division multiple access (TDMA), while the air-to-air link among UAVs using independent radio and channel by frequency division multiple access (FDMA).

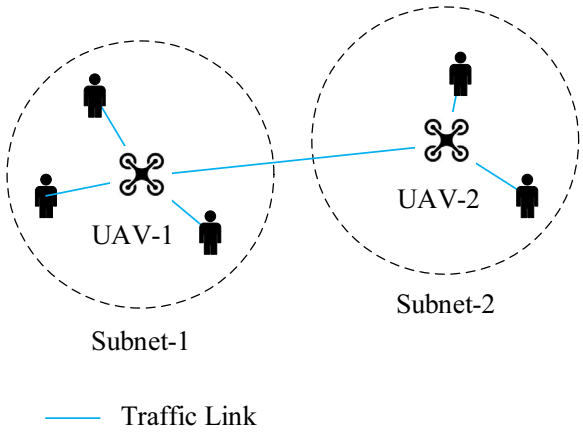

Figure 2. Top view of Group 1

- In a small area that may cause severe interference, all communication links, including those between drones and users, and those among drones, are allocated with resources in an orthogonal manner as described above, so it will not cause harmful interference; and in a larger area, it is possible to reuse spectrum resources between different areas without challenging interference, just like some cellular networks. In this way, harmful interference problems in the network can be avoided.
- Since the number of drones is less than the number of groups, the drones have to adopt a specific flight strategy to periodically meet the communication needs of each group. UAVs could provide relay services only when they are hovering at the intended location above a group. There is no service when UAVs are moving.
- Users can report their positions obtained by GPS to UAV. UAVs share the users' positions with each other through interactions that occupy little communication bandwidth.

In this paper, we consider a UAV-enabled communication network consisting of K UAVs denoted by $\mathcal{K} = \{k_1, k_2, ..., k_K\}$ flying at the same height of h.

The speed of each UAV is a constant v_A. The horizontal coordinates are denoted by $P_a = \{p_1, p_2, ..., p_K\}, p_i \in \mathbb{R}^2$. Drones are properly arranged to serve G groups ($G > K$) while each group has the number of g_i users on the ground. Users in group n can be represented as $U[n] = \{u_1[n], u_2[n], ..., u_{g_n}[n]\}$, all the users' positions are contained in $P_g = \{p_i[n] \in \mathbb{R}^2, \forall i, \forall n\}$ where $p_i[n]$ represents the position of user i in group n. UAVs employ two strategies for relaying as shown in Figure 3: (i). All UAVs serve a certain group at the same time (All UAVs to Each group, AE), and serve all groups by turns. (ii). Each drone serves different groups independently (Each to Each, EE), and each UAV will only be in charge of several groups and there is no group overlap. T_n^{hov} represents the duration UAVs hovered over group n, which also means the service time. T_{mn}^{fly} indicates the time consumed when UAVs move from group m to n. These two strategies focus on two different aspects: AE strategy aims to improve the relay quality while EE strategy aims to reduce the time consumption on flight. No matter which strategy is adopted, a UAV serving a certain group will hover at an optimal position.

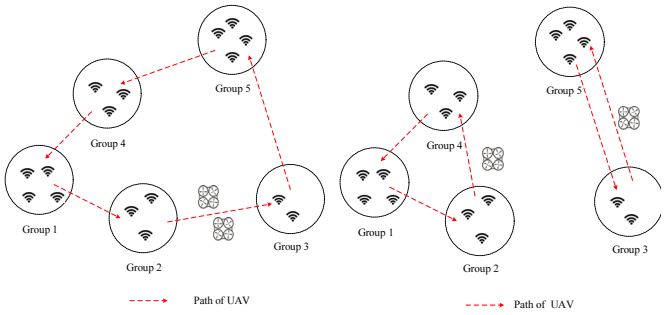

(a) (b)

Figure 3. Two UAVs employ AE and EE strategies for five groups

2.2 Transmission Model

2.2.1 Air-to-Ground Channel

The propagation channel of the air-to-ground link is modeled as [26], where the standard log-normal shadowing model is used to model the line-of-sight (LoS) and non-line-of-sight (NLoS) links by specific channel parameters. The LoS and NLoS path loss of UAV k_i and user $u_j[n]$ (in dB):

$$l_{k_i,u_j[n]}^{LoS} = L_{FS}(d_0) + 10\mu_{LoS}\log_{10}\left(d_{k_i,u_j[n]}\right) + \chi_{\sigma_{LoS}}, \quad (1)$$

$$l_{k_i,u_j[n]}^{NLoS} = L_{FS}(d_0) + 10\mu_{NLoS}\log_{10}\left(d_{k_i,u_j[n]}\right) + \chi_{\sigma_{NLoS}}, \quad (2)$$

where $d_{k_i,u_j[n]} = \sqrt{\| p_i - p_j[n] \|^2 + h^2}$ is the distance between UAV k_i and user $u_j[n]$. $L_{FS}(d_0)$ is the free space path loss which can be expressed by $20\log(d_0 f_c 4\pi/c)$. d_0 is the free-space reference distance while f_c is the carrier frequency and c is the speed of light. μ_{LoS} and μ_{NLoS} are the path loss exponents for LoS link and NloS link. $\chi_{\sigma_{LoS}}$ and $\chi_{\sigma_{NLoS}}$ are the shadowing random variables. Finally, for an air-to-ground link, the average path loss effect is expressed in dB as follows:

$$\overline{l}_{k_i,u_j[n]} = \Pr\left(l_{k_i,u_j[n]}^{LoS}\right) \times l_{k_i,u_j[n]}^{LoS} + \Pr\left(l_{k_i,u_j[n]}^{NLoS}\right) \times l_{k_i,u_j[n]}^{NLoS}, \quad (3)$$

where $\Pr\left(l_{k,u_i[t]}^{LoS}\right)$ is the air-to-ground link's probability to be a LoS link, and can be indicated by:

$$\Pr\left(l_{k_i,u_j[n]}^{LoS}\right) = \frac{1}{\left(1 + X\exp\left(-Y\left[\phi_{k_i,u_j[n]} - X\right]\right)\right)}, \quad (4)$$

where $\phi_{k_i,u_j[n]}$ is the elevation angle. And $\Pr\left(l_{k_i,u_j[n]}^{NLoS}\right) = 1 - \Pr\left(l_{k_i,u_j[n]}^{LoS}\right)$ is the probability to be a NLoS link. Based on the path loss, the average singal-to-noise ratio (SNR) of the channel between UAV k_i and user $u_j[n]$ is given by:

$$\gamma_{k_i,u_j[n]}^{G} = \frac{P}{10^{\overline{l}_{k_i,u_j[n]}/10}\sigma^2}, \quad (5)$$

where P is the transmit power and σ^2 is the variance of the Gaussian noise. The theoretic capacity of this channel will be:

$$r_{k_i,u_j}[n] = B\log_2\left(1 + \gamma_{k_i,u_j[n]}^{G}\right), \quad (6)$$

2.2.2 Air-to-Air Channel

Air-to-air links between different UAVs are considered as LoS links. Therefore, the path loss of an air-to-air channel between UAV k_i and UAV k_j can be expressed as:

$$\overline{l}_{k_i,k_j} = L_{FS}(d_0) + 10\mu_{LoS}\log_{10}\left(D_{k_i,k_j}\right) + \chi_{\sigma_{LoS}}, \quad (7)$$

where $L_{FS}(d_0)$, μ_{LoS} and $\chi_{\sigma_{LoS}}$ have the same meaning as above. $D_{k_i,k_j} = \sqrt{\| p_i - p_j \|^2}$ represents the spatial distance between two drones. The SNR of this channel is given by:

$$\gamma_{k_i,k_j}^{A} = \frac{P}{10^{\overline{l}_{k_i,k_j}/10}\sigma^2}, \quad (8)$$

and as the air-to-ground channel, the capacity of the air-to-air channel is:

$$R_{k_i,k_j}[n] = B\log_2\left(1 + \gamma_{k_i,k_j}^{A}\right), \quad (9)$$

2.3 UANET End-to-End Throughput

We assume the capacity of a single link is divided

equally by communications carried by the link. Considering decode-and-forward (DF), end-to-end throughput is equal to the capacity of the worst hop along the multi-hop route between two users. We hire a binary variable $a_{k_i,u_j}[n] \in \{0,1\}$ to express the connection between drones and users. $a_{k_i,u_j}[n]=1$ indicates UAV k_i and user $u_j[n]$ has a link. As the assumption 4 in section 2.1 states:

$$\sum_{i=1}^{K} a_{k_i,u_j}[n] \leqslant 1, \ \forall j, \forall n, \tag{10}$$

For a user's air-to-ground link, it's channel resources is shared through TDMA with other users' links within the same sub-network served by the same UAV. Each user's link can get $1/\theta_i$ time slot in a unit time, where $\theta_i = \sum_{j=1}^{g_n} a_{k_i,u_j}[n]$, is the number of users connected with UAV k_i. Then we get the real link rate:

$$\dot{r}_{k_i,u_j}[n] = \frac{r_{k_i,u_j}[n]}{\theta_i}, \tag{11}$$

between a UAV and a user. The link carries the number of $2(g_n-1)$ end-to-end communications, including the uplink and downlink transmissions to and from all the other users in group n. And for each communication, the available average rate is:

$$\overline{r}_{k_i,u_j}[n] = \frac{r_{k_i,u_j}[n]}{2\theta_i(g_n-1)}, \tag{12}$$

As for air-to-air links, the link capacity between UAV k_i and UAV k_j that both serve group n is denoted by $R_{k_i,k_j}[n]$ which could be calculated as (9). The link undertakes the cross-sub-networks communications with the number of $2\theta_i\theta_j$, and for each one the available rate is:

$$\overline{R}_{k_i,k_j}[n] = \frac{R_{k_i,k_j}[n]}{2\theta_i\theta_j}, \tag{13}$$

We consider a communication between $u_i[n]$ and $u_j[n]$ which are both connected with UAV k_1, the end-to-end throughput can be expressed as:

$$J_{ij}[n] = \min\left(\overline{r}_{k_1,u_i}[n], \overline{r}_{k_1,u_j}[n]\right), \tag{14}$$

Similarly, we can get the end-to-end throughput between $u_i[n]$ and $u_j[n]$, which are connected to UAVs k_1 and k_2 respectively, as:

$$J_{ij}[n] = \min\left(\overline{r}_{k_1,u_j}[n], \overline{R}_{k_1,k_2}[n], \overline{r}_{k_2,u_j}[n]\right), \tag{15}$$

The sum of end-to-end throughput of user $u_i[n]$ can be expressed as follows:

$$J_i[n] = \sum_{j=1}^{g_n} J_{ij}[n], \tag{16}$$

On the basis of the above formulas, the total throughput of group n is the sum of end-to-end throughput of all users, which can be represented by:

$$\begin{aligned} J[n] &= \sum_{i=1}^{g_n} J_i[n], \\ &= \sum_{i=1}^{g_n} \sum_{\substack{j=1 \\ j\neq i}}^{g_n} J_{ij}[n], \end{aligned} \tag{17}$$

In this section, we described the model and got the total throughput of each group. However, it is a non-convex smooth function. In the next section, we will show the problems to be optimized.

3 Problem Formulation

UAVs aim to serve the G groups properly and they could employ AE or EE strategy as stated in the previous section for different occasions. With both AE and EE, UAVs provide relay services for groups periodically, T denotes the duration of each cycle in second (s). The two different service strategies lead to two different formulaic models, but the essence of them is the same. Next, we will introduce the models in detail.

3.1 Problem Formulation of AE Strategy

AE strategy requires UAVs to work together. In each duration, the network throughput maximization problem can be formulated as follows[1]:

$$\text{(P1)}: \max_{P_a, \pi_{mn}} \ \eta \tag{18a}$$

Subject to:

$$\frac{1}{\omega_n T} J[n] T_n^{hov} \geqslant \eta, \ \forall n, \tag{18b}$$

$$\sum_{\substack{m=1 \\ m\neq n}}^{G} \pi_{nm} \leqslant \sum_{\substack{m=1 \\ m\neq n}}^{G} \pi_{mn}, \ \forall n, \tag{18c}$$

$$\sum_{\substack{m=1 \\ m\neq n}}^{G} \pi_{mn} \leqslant 1, \ \forall n, \ \sum_{\substack{n=1 \\ n\neq m}}^{G} \pi_{mn} \leqslant 1, \ \forall m, \tag{18d}$$

$$\pi_{mn} + \pi_{nm} \leqslant 1, \quad \forall m, \forall n, \tag{18e}$$

$$\sum_{n=1}^{G} T_n^{hov} + \sum_{\substack{m=1 \\ m\neq n}}^{G} \sum_{n=1}^{G} \pi_{mn} T_{mn}^{fly} \leqslant T, \tag{18f}$$

where (i) π_{mn}: a binary variable identifying the path of UAVs (i.e., $\pi_{mn}=1$ indicates UAVs will serve group n directly after m). (ii) As mentioned above, T_n^{hov} denotes the service time of group n while T_{mn}^{fly} is the

time consumed by UAVs when moving from group m to n. (iii) ω_n is a parameter indicating the weights of group n where a higher value of ω_n will result in longer service time.

Constraint (18c) ensures that UAVs can leave group n only if it has already arrived there. Constraint (18d) force the UAVs to serve at most one new group when leaving its current group. Constraint (18e) prohibits UAVs returning to a node that it just left. Constraint (18f) is the limitation of the cycle T, which is large enough to make sure that each serving time T_n^{hov} can be a positive number.

P1 is the formulation of AE strategy which indicates that our goal is to maximize the minimal weighted throughput of all groups. It reflects the consideration of the balancing between importance and fairness, where a group in an urgent situation can increase its weight factor appropriately.

3.2 Problem Formulation of EE Strategy

With EE strategy applied, each UAV is in charge of different groups. A new binary variable π_{mnd} is employed, where $\pi_{mnd}=1$ indicates that UAV k_d will serve group n directly after m. The problem can be formulated as follows[2]:

$$\text{(P2)}: \max_{P_d, \pi_{mnd}} \quad \eta \tag{19a}$$

Subject to:

$$\frac{1}{\omega_n T} J[n] T_n^{hov} \geq \eta, \ \forall n, \tag{19b}$$

$$\sum_{\substack{m=1 \\ m\neq n}}^{G} \pi_{mnd} \leq \sum_{\substack{m=1 \\ m\neq n}}^{G} \pi_{nmd}, \forall n, \forall d, \tag{19c}$$

$$\begin{aligned} &\sum_{\substack{m=1 \\ m\neq n}}^{G} \pi_{mnd} \leq 1, \ \forall n, \forall d, \\ &\sum_{\substack{n=1 \\ n\neq m}}^{G} \pi_{mnd} \leq 1, \ \forall m, \forall d, \end{aligned} \tag{19d}$$

$$\sum_{\substack{m=1 \\ m\neq n}}^{G} \sum_{d=1}^{K} \pi_{mnd} = 1, \ \forall n, \tag{19e}$$

$$\sum_{\substack{m=1 \\ m\neq n}}^{G} \sum_{n=1}^{G} \pi_{mnd} (T_n^{hov} + T_{mn}^{fly}) \leq T, \ \forall d, \tag{19f}$$

The constrains (19b) (19c) (19d) and (19f) have the same meaning as AE strategy, and are the restrictions of each drone. A new constraint (19e) indicates each group can only by served by one UAV within a cycle, where we lift the restriction in AE that drones cannot fly back and forth between two groups. The drones, serving different groups respectively at the same time, use orthogonal resources for communications in TDMA/FDMA, so the SNR model proposed above is still available.

P1 and P2 are classified as mixed integer non-linear programming problems (MINLP) because the throughput of each group is considered as a non-convex function, where the optimal solution is difficult to obtain. Therefore, in the next section, we divide the solution process into two steps aiming to find an efficient solution for UAVs' management. Note that the choice of T has a significant impact on the system performance, a short cycle may not be enough to support the UAVs' flight time, therefore, we define T long enough for the flight time of all UAVs.

4 Proposed Algorithm

P1 and P2 raised in section 3 are UAVs' trajectory optimization problems. However, it is difficult to solve the problems directly, we propose an algorithm aiming to solve two sub-problems of both P1 and P2 in two steps, which are (i): figuring out the best hovering positions for UAVs when providing services. (ii): designing the service order and service time of each group reasonably. Although the AE and EE strategies are not exactly the same, the core idea of our proposed algorithm works for both.

4.1 Hovering Position Determination of UAVs

When drones serve specific groups, we propose a distributed gradient-based control algorithm, which is designed to drive each UAV along the gradient direction of the global objective function, to optimize the total end-to-end throughput of each group. With the process of these movements, the overall target can be optimized. As a result of the local non-differentiability of the objective function, we use generalized gradient instead. The stability of the algorithm is further proved by non-smooth analysis.

To provide communication for a user group, we need to determine the specific users served in each drone's subnet. Based on the user's geographic location and business needs, we could reasonably divide the sub-networks.

4.1.1 Generalized Gradient Controller

Gradient descent (ascent) is a general method to solve various engineering optimization problems. In Figure 4, we consider an iterative optimization process using gradient ascent, which can be expressed as:

$$p_{k+1} = p_k + \lambda g(p_k), \tag{20}$$

where p_k represents the variable at the k^{th} iteration,

$\lambda > 0$ is the iteration step and $g(p_k)$ indicates the gradient of objective function at p_k.

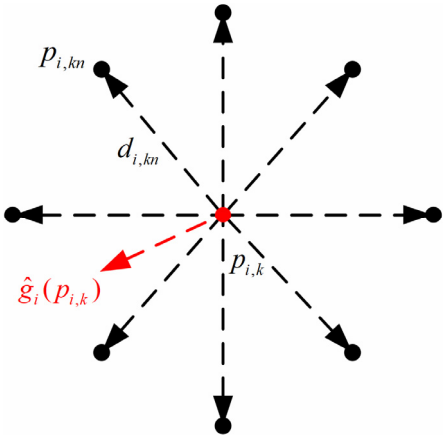

Figure 4. An example of sample points and vectors around a control point

1. For readability, we use the following notations $\forall m$ and $\forall n$ to denote $\forall m = 1,...,G,$ and $\forall n = 1,...,G,$.

2. We use the notation $\forall d$ to denote $\forall d = 1,...,K,$. $\forall m$ and $\forall n$ have the same meaning as 1.

Due to the existence of minimum functions in (17) lead to locally non-differentiable at points where the elements in minimum function are equal, we must use the generalized gradient and next we will show how it works. To simplify the expression, J is used to represent the total throughput of each group $J[n], \forall n \in G$.

In [20], for a local Lipschitz function J, $\mathbb{R}^d \to \mathbb{R}$. The generalized gradient ∂J at a non-differentiable point p, can be expressed as the convex hull of all possible limits of the gradient at neighboring points where the function J is differentiable in [23]. Otherwise, the generalized gradient $\partial J(p) = \nabla J(p)$. And the generalized gradient vector field $Ln(\partial J)$, $\mathbb{R}^d \to \mathbb{R}$, where $Ln: \mathfrak{B}(\mathbb{R}^d) \to \mathfrak{B}(\mathbb{R}^d)$ is a set-valued map that associates to each subset S of $\mathbb{R}^d$, the set of least-norm elements of its closure $\overline{S}$. Furthermore, $Ln(\partial J / \partial p)$ is an ascent direction of J at $p \in \mathbb{R}^d$.

Then, we design generalized gradient controllers, for UAV i, the controller can be expressed as:

$$\dot{p}_i = Ln(\partial J)(p_i), \tag{21}$$

where $Ln(\partial J)$ is the generalized gradient vector field of J, and p_i is the position of UAV i.

The calculation of generalized gradients is difficult. In this paper, we use a stochastic approximation approach named least squares gradient estimation (LSGE) in [31]. The algorithm uses the least square method to fit the objective function and gives the estimation of generalized gradient to the target point.

We take n sample points $\{p_{i,k_1}, p_{i,k_2}, ..., p_{i,k_n}\}$ around the position of UAV i at $p_{i,k}$ (defined as control point) of time k with sample angle $2\pi/n$ and define the sample vector:

$$\vec{d}_{i,k_n} = p_{i,k_n} - p_{i,k}, \tag{22}$$

where $\vec{d}_{i,k_n} = e\vec{v}_{i,k}$, with $\|\vec{v}_{i,k}\| = 1$ is the vector direction and $e > 0$ is the length of sample vector. Define the sample matrix $H_{i,k}$:

$$H_{i,k} = \begin{bmatrix} 1 & \vec{d}_{i,k_1} \\ \vdots & \vdots \\ 1 & \vec{d}_{i,k_n} \end{bmatrix}, \tag{23}$$

then the LSGE method is given by:

$$\begin{bmatrix} \hat{J}(p_{i,k}) \\ \hat{g}_i(p_{i,k}) \end{bmatrix} = (H_{i,k}^T H_{i,k})^{-1} H_{i,k}^T \begin{bmatrix} J(p_{i,k_1}) \\ \vdots \\ J(p_{i,k_n}) \end{bmatrix}, \tag{24}$$

where $\hat{J}(p_{i,k})$ is an estimate value of the objective function, $\hat{J}(p_{i,k_n})$ denotes the measurement of objective function at sample point p_{i,k_n}, which can be precisely calculated as the positions of all other nodes can be obtained in real time. $\hat{g}_i(p_{i,k})$ is the estimation of generalized gradient of UAV i at $p_{i,k}$. The error and variance analysis of this method in estimating the generalized gradient was presented in [31].

Using the generalized gradient estimation method, the position iteration process for UAV i can be expressed as:

$$p_{i,k+1} = p_{i,k} + \alpha_{i,k} g_i(p_{i,k}), \tag{25}$$

where $\alpha_{i,k}$ is used to control the position adjustment for UAV i in k^{th} iteration.

4.1.2 Non-smooth Analysis of the Controller

Here we present the stability analysis of generalized gradient controller in equation (21), and achieve this by non-smooth analysis in discontinuous dynamic system [30].

The existence of generalized gradient vector field of the objective function depends on the fact that the function is locally Lipschitz and regular. If a function is continuously differentiable at x, it is locally Lipschitz and regular at x. Relevant concepts was introduced in [30].

There are some properties that can help to conserve the locally Lipschitz and regular property of objective function. We refer to the Dilation Rule, Sum Rule given in [30] in part "Computing the Generalized Gradient" and the properties provided in [30] Proposition 7.

Theorem: UAVs follow the generalized gradient vector field of J such that $\dot{p}_i = Ln(\partial J / \partial p_i)$ will asymptotically converge to the critical points of J where the strongly stable critical points are local maxima of J.

Proof: As the basic element equation (6) and (9) of J is continuously differentiable in the deployment area, equation (14) and (15) are locally Lipschitz and regular using the Proposition 7 in [30]. Then, consider the objective function J, which is an algebraic composition of a series of minimum functions, by applying the Dilation Rule and Sum Rule, we conclude that J is locally Lipschitz and regular. According to Proposition 11 in [23], the strict maximizer of J are strongly equilibria of the non-smooth gradient flow of J. Further, we find a compact and strongly invariant set for this dynamic system following the example of [31]. If the UAV flies out of the ground user field, it will fail to communicate with other nodes which leads to the generalized gradient $\partial J / \partial p_i$ for agent i goes to zero. Therefore, the ground user field is a strongly invariant set that with any initial conditions, the UAV will converge to the set of critical points of J.

Solving the hovering problem, we can determine the best positions for UAVs of each group. We define $P_{AE}^{hov}[n] = \{p_1^{hov}[n], ..., p_K^{hov}[n],\ p_i^{hov}[n] \in \mathbb{R}^2\}$ for AE strategy and $P_{EE}^{hov}[n] = \{p_{EE}^{hov}[n] \in \mathbb{R}^2\}$ for EE strategy.

4.2 Joint Design of Trajectory and Service Time

Generalized gradient controller helps to maximize the throughput of each group. Due to the value of function (18b) and (19b) are decided by both throughput and service time, this subsection intends to optimize the latter. We will discuss the joint designed methods corresponding to the AE and EE strategies.

4.2.1 Joint Design for AE Strategy

AE strategy contains only one same path for all UAVs, it is obvious that increasing the total service time of all groups equals to increasing the service time of each group. Firstly, we aim to improve the total service time which can be expressed as:

$$\max_{\pi_{mn}} \quad \sum_{n=1}^{G} T_n^{hov} \tag{26}$$

Subject to:

(18b), (18c), (18d), (18e) and (18f).

Only constraint (18f) limits service time direcly, and the other four constraints aim to restrict path of UAVs which will not have any impact on constraints (18f). Therefore it is easy to understand when (26) is optimal, the left side of constraints (18f) should equal to the right. The problem (26) can be reformulated as follows:

$$\text{(P3): min} \quad \sum_{m=1}^{G}\sum_{n=1}^{G} \pi_{mn} T_{mn}^{fly} \tag{27}$$

Subject to:

(18b), (18c), (18d) and (18e).

In fact, once we get the hovering locations where the UAVs provide relay services, the time consumption of flight between two groups, T_{mn}^{fly}, can be determined as follows:

for AE strategy:

$$\begin{aligned} T_{mnd}^{fly} &= \frac{\| p_{AE}^{hov}[m] - p_{AE}^{hov}[n] \|}{v_A}, \\ T_{mn}^{fly} &= \max_{\forall d \in \mathcal{K}} (T_{mn1}^{fly}, T_{mn2}^{fly}, ..., T_{mnK}^{fly}), \end{aligned} \tag{28}$$

For EE strategy:

$$T_{mn}^{fly} = \frac{\| p_{EE}^{hov}[m] - p_{EE}^{hov}[n] \|}{v_A}, \tag{29}$$

where T_{mnd}^{fly} representes the flight time of UAV d from group m to n. (28) means, when changing group, time consumption is detemined by the longest flight time of all the UAVs.

(P3) is to determine the path for UAVs, where the only variable is π_{mn} whose value could be 0 or 1. It is 0-1 integer programming problem which can be solved optimally using software like CPLEX [32].

We get an optimized total service time of all groups after solving P3, the final goal to maximize the minimal weighted throughput of each group can be expressed as:

$$\text{(P4): max} \quad \eta \tag{30a}$$

Subject to:

$$\frac{1}{\omega_n T} J[n] T_n^{hov} \geqslant \eta, \ \forall n, \tag{30b}$$

$$\sum_{n=1}^{G} T_n^{hov} \leqslant C, \tag{30c}$$

where C is a constant because the cycle time T, flight time T_{mn}^{fly} and UAVs' service order π_{mn} have been identified. The problem P4 is a standard Linear programming problem (LP) which is easy to solve, and the joint design of trajectory and service time is then determined. Since the best hover position leads to the maximum throughput for each group as mentioned before, finally our initial problem P1 is optimized.

4.2.2 Trajectory Design for EE Strategy

As for EE strategy, the increase of total service time for all groups doesn't necessarily lead to the increase for each group, because each UAV is in charge of different groups, which means that UAVs are not

completely independent. We can't separate this problem into two parts like in AE. But for UAV d, when its trajectory π_{mnd} is determined, the service time allocation problem is a LP like P4, so the optimal problem can be determined as:

$$\text{(P5):} \max_{P_a, \pi_{mnd}} \quad \eta_d \tag{31a}$$

Subject to:

$$\frac{1}{\omega_n T} J[n] T_n^{hov} \geq \eta_d \sum_{m=1}^{G} \pi_{mnd}, \ \forall n, \tag{31b}$$

$$\sum_{m=1}^{G} \sum_{n=1}^{G} \pi_{mnd} (T_n^{hov} + T_{mn}^{fly}) \leq T, \ \forall d, \tag{31c}$$

where η_d is the optimized throughput of the groups in the charge of UAV d. The η in P2 is the minimum value of all η_d where $\eta = \min_{\forall d \in \mathcal{K}} (\eta_1, \eta_2, ..., \eta_K)$.

The problem P2 is a MILP where the variables π_{mnd} are integer binary variables and T_n^{hov} is continuous. To solve this problem, some method with higher computation complexity, like branch and bound method, could be employed. However, some software can still achieve the optimal result quickly when the system scale is not very huge.

The problems P1 and P2 for AE and EE have been solved in this section, and we get the best hover position, trajectory and service time allocation for each UAV. However, the result may not be the global optimal solution. UAVs can perform well at the best hovering position, but if we move the hovering position of the UAVs slightly toward the next group, the throughput $J[n]$ will decrease, the flight time between groups will decrease as well, which means the service time may grow accordingly. This phenomenon is more obvious when UAVs' flying speed is low or the cycle T is short. With the cycle T increasing, this effect gradually diminishes until finally disappears. It will take much more time to search the global optimal result, which may not be so attractive to achieve very little throughput gain. Even though our proposed algorithm in this section may only get a sub-optimal result, it is acceptable and computationally economical. The numerical results and discussion will be shown in the next section.

5 Numerical Results and Discussion

In this section, we show the performance of the proposed algorithm to optimize the weighted throughput of all groups.

The algorithm is implemented on MATLAB and the simulation parameters are provided in Table 1.

Table 1. Simulation parameters

Parameter	Value	Parameter	Value
h	100m	μ_{LoS}	2
B	10MHz	μ_{NLoS}	2.4
P	1W	$\chi_{\sigma_{LoS}}$	5.3
v_A	30m/s	$\chi_{\sigma_{NLoS}}$	5.27
σ^2	-110dBm	X	11.9
d_0	5m	Y	0.13
f_c	30GHz	T	400~2000s

Firstly, the effect of the gradient-based algorithm (GBA) determining UAVs' hovering positions is shown in Figure 5, which presents three scenarios, with 2 drones for 4 users (Scenario a), 3 drones for 8 users (Scenario b), and 4 drones for 11 users (Scenario c), in a 3000m * 3000m area. GBA drives the UAVs along the generalized gradient flow and stops at positions marked with stars. The change of system throughput during the optimization process is shown in Figure 6, increasing from 5.8955 to 24.0237Mbps (Scenario a), 16.6945 to 66.8543Mbps (Scenario b) and 30.9858Mbps to 129.6988Mbps (Scenario c). The UAVs' final convergent positions are the same even with different initial positions.

Particle swarm optimization (PSO) [28] is a heuristic iteration algorithm, which can obtain global optimal solution with multiple particles joint searching solution space. Let P_{num} be the particle number, N denotes the UAV number, I denotes the iteration times, F represents the cost of calculating the fitness function in each iteration. So the total complexity of PSO is $NP_{num}IF$. For GBA, the total complexity is $P_k IF$, where P_k denotes the number of sampling points when the drone calculates the gradient. Generally, the value of P_k is 4 or 8. Obviously, the GBA has a significant advantage of lower complexity compared to PSO.

Figure 7 intuitively demonstrates the performance difference of the two algorithms. Scenario (a) contains 10 independent simulations with 3-UAVs and 8-users and scenario (b) contains 10 independent simulations with 6-UAVs and 14-users. We can observe a great improvement in system throughput by using GBA. The final results of our method are very close to PSO, verifying that our algorithm can obtain optimal positions in theory. In these 20 sample scenarios, the average deviation of system throughput of GBA with respect to PSO optimal value is lower than 0.1%.

In Figure 8, we consider two scenarios, 2 UAVs serving 5 groups and 3 UAVs serving 7 groups, in a 4000m * 4000m area. In both scenarios, the flight cycle duration T = 700s. Each group has different number of users with an average of 5. Two kinds of serving strategies are applied in both scenarios, AE in Figure 8 (a) and Figure 8(c), EE in Figure 8(b) and

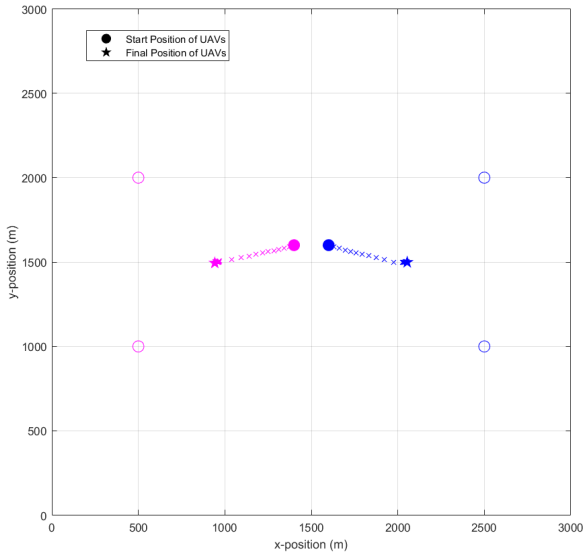

(a)

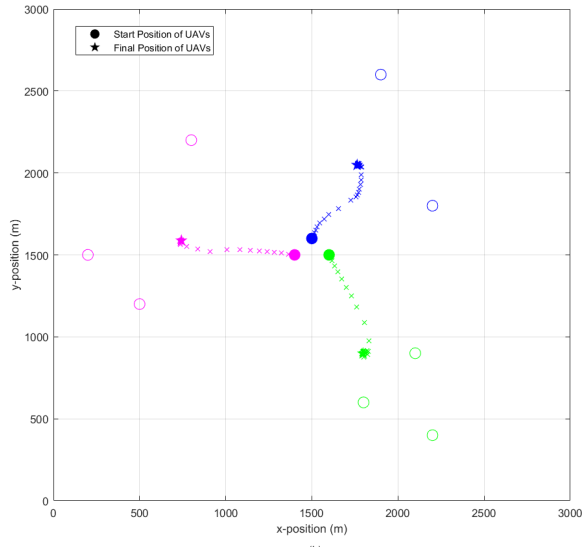

(b)

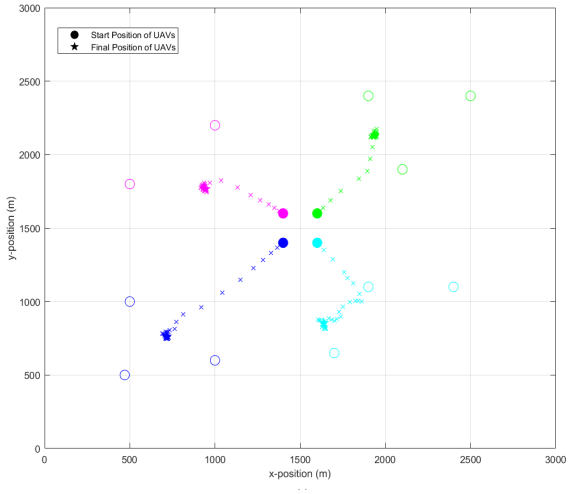

(c)

Figure 5. The optimization of three sample scenarios

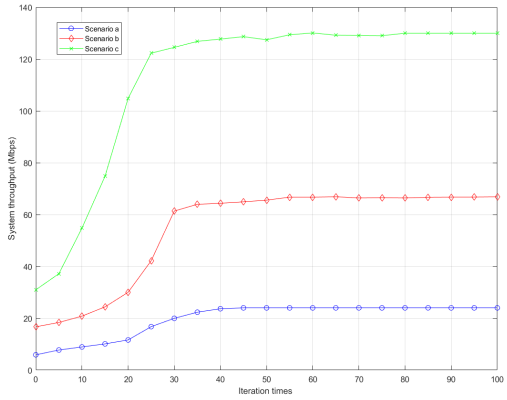

Figure 6. Variation of throughput versus iteration times

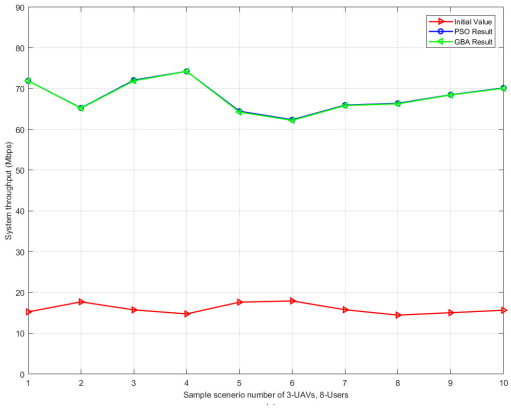

(a)

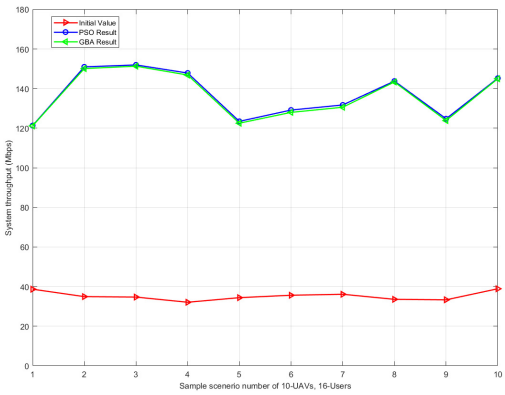

(b)

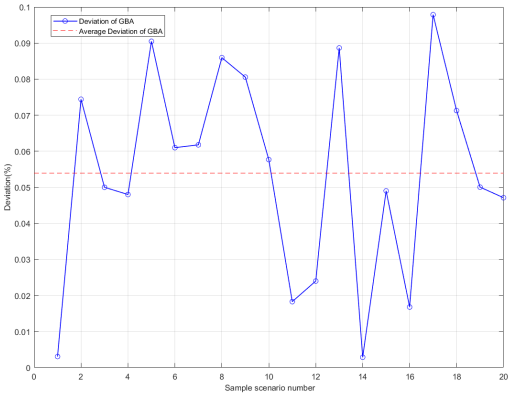

(c)

Figure 7. Comparison of GBA and PSO in optimization performance

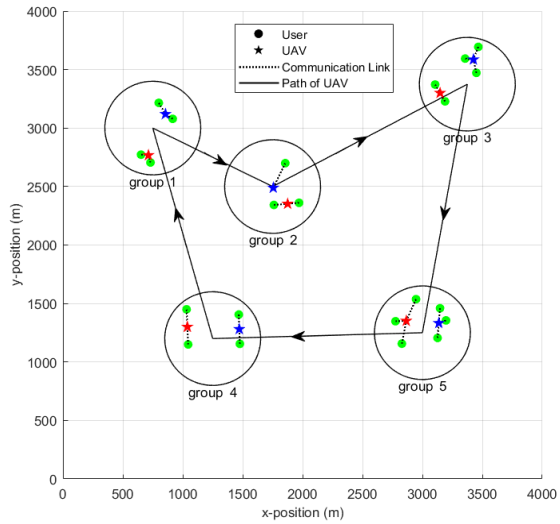

(a) $K = 2$, $G = 5$ using AE strategy

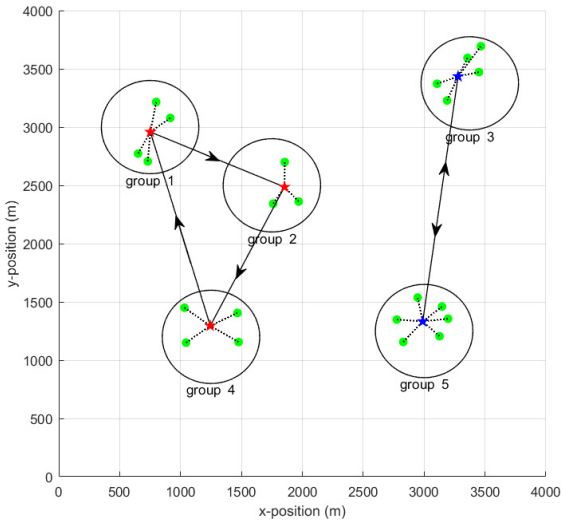

(b) $K = 2$, $G = 5$ using EE strategy

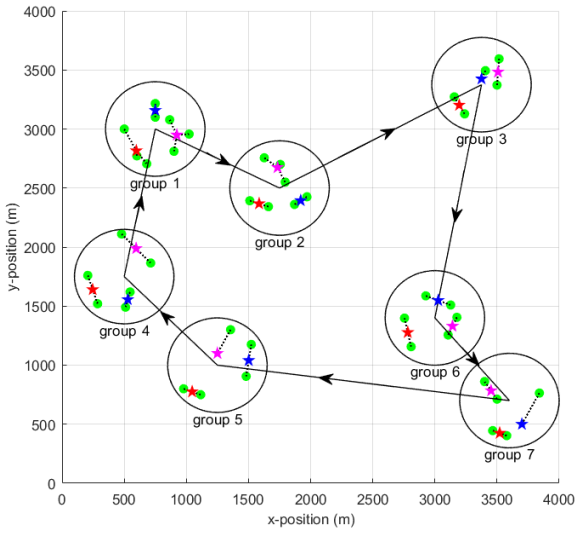

(c) K =3, $G = 7$, using AE strategy

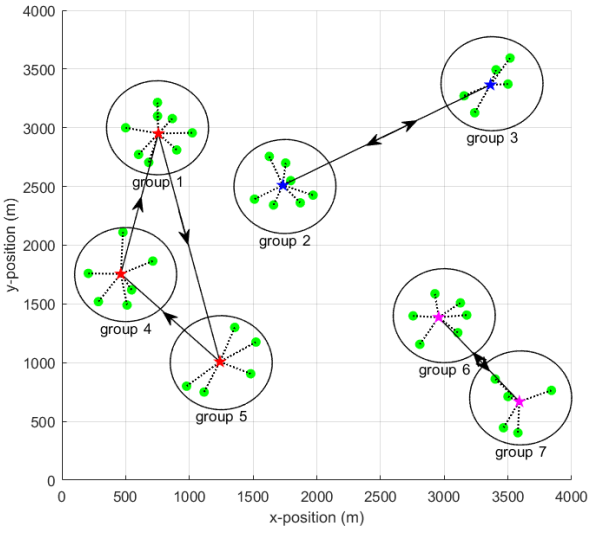

(d) $K = 3$, $G = 7$ using EE strategy

Figure 8. Optimized trajectories

Figure 8(d). The hovering positions of UAVs for each group are obtained by GBA to improve throughput when serving. With AE strategy, UAVs act in unison and provide relay services for all groups by turns. Each UAV forms a sub-network contains several users when serving, the number of users in each sub-network are almost the same. With EE strategy, each UAV only need to serve several groups, while establishing communication links with all the users in one group. The optimized trajectories using MILP solution are plotted in Figure 8.

Figure 9 is the throughput comparison with different cycle durations between two strategies. We change the flight cycle from 400 to 2000 seconds. The 2 UAVs and 5 user's scenario mentioned in Figure 8(a) and Figure 9(b) is selected. It is obvious that the throughput of both strategies increases with T, and EE performs better than AE. When T is relatively low, the performance gap between the two strategies is more significant.

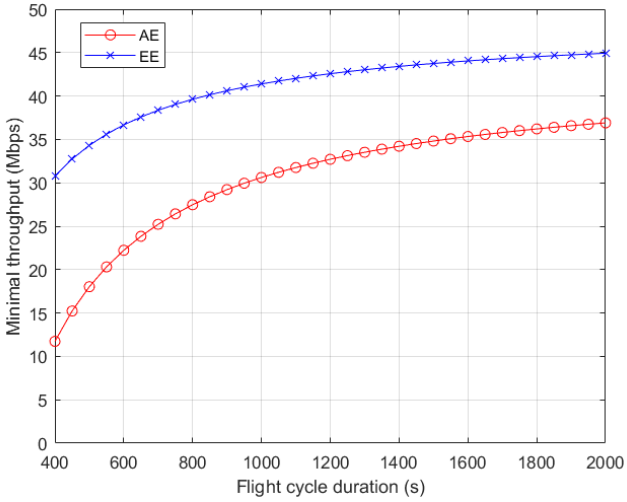

Figure 9. Comparison between AE and EE strategies in different flight cycle

Figure 10 shows the effect of different numbers of UAVs, in a larger 8000m * 8000m area with 12 groups on the ground. Each group has 8 users in average and the distance between every two adjacent groups is around 1500m. As the number of UAVs grows from 1 to 6, the average throughput of EE strategy increases much faster than AE strategy.

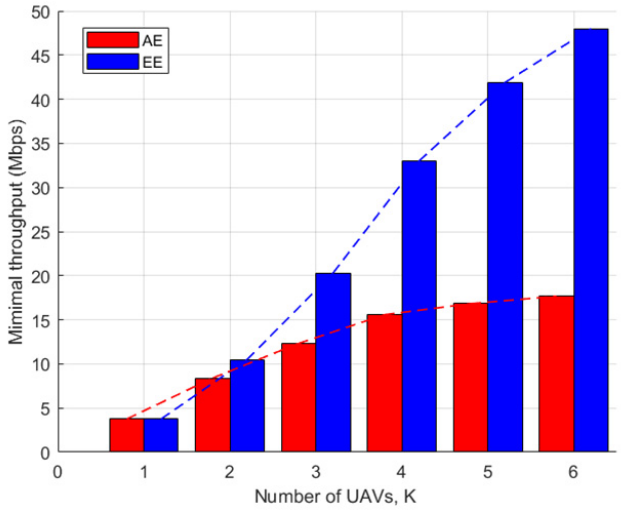

Figure 10. Comparison between AE and EE strategies in different number of UAVs

To explore the impact of unexpected conditions on the system, Figure 11 shows a case that during the service period a drone suddenly malfunctions and fails to serve, in a 2000m * 2000m area with 10 users served by different number of UAVs. The green bars are the throughput when all UAVs work normally, and the purple bars when a UAV fails. It is reasonable that the stability of the system is higher when more drones are available. If there is only one serving UAV, the system is extremely fragile, which indicates AE strategy is more robust than EE.

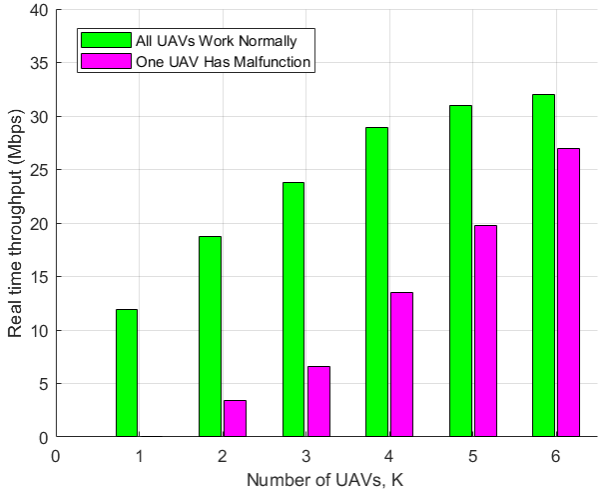

Figure 11. Effect on real-time throughput when a UAV has malfunction

6 Conclusion

In this paper, we designed a joint trajectory and resource allocation algorithm for UAV-enabled networks to provide communication for ground users in emergency scenarios. The solutions for both AE and EE serving strategies are studied, containing the design of hovering positions, path of UAVs and service time allocation. The generalized gradient-based algorithm ensures the UAV deploys adaptively to maximize the throughput of a group in service. The remaining problem is separated into a MILP for the best flight trajectory and a LP to optimally allocate the service time. The effectiveness of our proposed algorithm has been verified by extensive simulation results, also showing EE strategy has a better performance in terms of throughput while AE strategy has a greater robustness in case of drone malfunction.

Acknowledgements

This work was supported in part by the Beijing Natural Science Foundation (L192002) and the National Natural Science Foundation of China (No. 61631004 and No. 61971058).

References

[1] Y. Zeng, R. Zhang, T. J. Lim, Wireless Communications with Unmanned Aerial Vehicles: Opportunities and Challenges, *IEEE Communication Magazine*, Vol. 54, No. 5, pp. 36-42, May, 2016.

[2] H. Gao, C. Liu, Y. Li, X. Yang, V2VR: Reliable Hybrid-Network-Oriented V2V Data Transmission and Routing Considering RSUs and Connectivity Probability, *IEEE Transactions on Intelligent Transportation Systems*, early access, April, 2020, DOI: 10.1109/TITS.2020.2983835.

[3] S. Deng, Z. Xiang, P. Zhao, J. Taheri, H. Gao, J. Yin, A. Y. Zomaya, Dynamical Resource Allocation in Edge for Trustable Internet-of-Things Systems: A Reinforcement Learning Method, *IEEE Transactions on Industrial Informatics*, Vol. 16, No. 9, pp. 6103-6113, September, 2020.

[4] H. Gao, W. Huang, Y. Duan, The Cloud-Edge Based Dynamic Reconfiguration to Service Workflow for Mobile Ecommerce Environments: A QoS Prediction Perspective, *ACM Transactions on Internet Technology*, 2020, DOI: 10.1145/3391198.

[5] X. Ma, H. Gao, H. Xu, M. Bian, An IoT-Based Task Scheduling Optimization Scheme Considering the Deadline and Cost-Aware Scientific Workflow for Cloud Computing, *EURASIP Journal on Wireless Communications and Networking*, Vol. 2019, No. 1, Article number: 249, November, 2019, DOI: 10.1186/s13638-019-1557-3.

[6] H. Gao, Y. Xu, Y. Yin, W. Zhang, R. Li, X. Wang, Context-Aware QoS Prediction with Neural Collaborative Filtering for Internet-of-Things Services, *IEEE Internet of Things Journal*,

Vol. 7, No. 5, pp. 4532-4542, May, 2020.

[7] X. Yang, S. Zhou, M. Cao, An Approach to Alleviate the Sparsity Problem of Hybrid Collaborative Filtering Based Recommendations: The Product-Attribute Perspective from User Reviews, *Mobile Networks and Applications*, Vol. 25, No. 2, pp. 376-390, April, 2020.

[8] H. Gao, L. Kuang, Y. Yin, B. Guo, K. Dou, Mining Consuming Behaviors with Temporal Evolution for Personalized Recommenddation in Mobile Marketing Apps, *Mobile Networks and Applications*, Vol. 25, No. 4, pp. 1233-1248, August, 2020.

[9] M. Mozaffari, W. Saad, M. Bennis, M. Debbah, Drone Small Cells in the Clouds: Design, Deployment and Performance Analysis, *2015 IEEE Global Communications Conference (GLOBECOM)*, San Diego, CA, 2015, pp. 1-6.

[10] M. Mozaffari, W. Saad, M. Bennis, M. Debbah, Efficient Deployment of Multiple Unmanned Aerial Vehicles for Optimal Wireless Coverage, *IEEE Communications Letters*, Vol. 20, No. 8, pp. 1647-1650, August, 2016.

[11] D. G. Reina, H. Tawfik, S. L. Toral, Multi-subpopulation Evolutionary Algorithms for Coverage Deployment of UAV-networks, *Ad Hoc Networks*, Vol. 68, pp. 16-32, January, 2018.

[12] Z. Han, A. L. Swindlehurst, K. J. R. Liu, Optimization of MANET Connectivity via Smart Deployment/Movement of Unmanned Air Vehicles, *IEEE Transactions on Vehicular Technology*, Vol. 58, No. 7, pp. 3533-3546, September, 2009.

[13] H. Ghazzai, M. B. Ghorbel, A. Kassler, M. J. Hossain, Trajectory Optimization for Cooperative Dual-Band UAV Swarms, *2018 IEEE Global Communications Conference (GLOBECOM)*, Abu Dhabi, United Arab Emirates, 2018, pp. 1-7,.

[14] M. Chen, M. Mozaffari, W. Saad, C. Yin, M. Debbah, C. S. Hong, Caching in the Sky: Proactive Deployment of Cache-Enabled Unmanned Aerial Vehicles for Optimized Quality-of-Experience, *IEEE Journal on Selected Areas in Communications*, Vol. 35, No. 5, pp. 1046-1061, May, 2017.

[15] Y. Wang, M. Chen, Z. Yang, T. Luo, W. Saad, Deep Learning for Optimal Deployment of UAVs with Visible Light Communications, *IEEE Transactions on Wireless Communications*, early access, July, 2020, DOI: 10.1109/ TWC. 2020.3007804.

[16] Q. Wu, Y. Zeng, R. Zhang, Joint Trajectory and Communication Design for Multi-UAV Enabled Wireless Networks, *IEEE Transactions on Wireless Communications*, Vol. 17, No. 3, pp. 2109-2121, March, 2018.

[17] C. Zhan, Y. Zeng, R. Zhang, Energy-Efficient Data Collection in UAV Enabled Wireless Sensor Network, *IEEE Wireless Communications Letters*, Vol. 7, No. 3, pp. 328-331, June, 2018.

[18] X. Liu, Y. Liu, Y. Chen, L. Hanzo, Trajectory Design and Power Control for Multi-UAV Assisted Wireless Networks: A Machine Learning Approach, *IEEE Transactions on Vehicular Technology*, Vol. 68, No. 8, pp. 7957-7969, August, 2019.

[19] C. Dixon, Controlled Mobility of Unmanned Aircraft Chains to Optimize Network Capacity in Realistic Communication Environments, Ph.D. Thesis, *University of Colorado at Boulder*, Boulder, Colorado, 2010.

[20] C. Dixon, E. W. Frew, Optimizing Cascaded Chains of Unmanned Aircraft Acting as Communication Relays, *IEEE Journal on Selected Areas in Communications*, Vol. 30, No. 5, pp. 883-898, June, 2012.

[21] Y. Sun, D. Xu, D. W. K. Ng, L. Dai, R. Schober, Optimal 3D-Trajectory Design and Resource Allocation for Solar-Powered UAV Communication Systems, *IEEE Transactions on Communications*, Vol. 67, No. 6, pp. 4281-4298, June, 2019.

[22] M. Mozaffari, A. T. Z. Kasgari, W. Saad, M. Bennis, M. Debbah, Beyond 5G With UAVs: Foundations of a 3D Wireless Cellular Network, *IEEE Transactions on Wireless Communications*, Vol. 18, No. 1, pp. 357-372, January, 2019.

[23] Y. Zeng, R. Zhang, T. J. Lim, Throughput Maximization for UAV-Enabled Mobile Relaying Systems, *IEEE Transactions on Communications*, Vol. 64, No. 12, pp. 4983-4996, December, 2016.

[24] V. Sharma, I. You, J. T. Seo, M. Guizani, Secure and Reliable Resource Allocation and Caching in Aerial-Terrestrial Cloud Networks (ATCNs), *IEEE Access*, Vol. 7, pp. 13867-13881, January, 2019.

[25] S. ur Rahman, G. Kim, Y. Cho, A. Khan, Positioning of UAVs for Throughput Maximization in Software-defined Disaster Area UAV Communication Networks, *Journal of Communications and Networks*, Vol. 20, No. 5, pp. 452-463, October, 2018.

[26] R. Ghanavi, E. Kalantari, M. Sabbaghian, H. Yanikomeroglu, A. Yongacoglu, Efficient 3d Aerial Base Station Placement Considering Users Mobility by Reinforcement Learning, *2018 IEEE Wireless Communications and Networking Conference (WCNC)*, Barcelona, Spain, 2018, pp. 1-6.

[27] M. Chen, U. Challita, W. Saad, C. Yin, M. Debbah, Artificial Neural Networks-Based Machine Learning for Wireless Networks: A Tutorial, *IEEE Communications Surveys & Tutorials*, Vol. 21, No. 4, pp. 3039-3071, Fourth Quarter, 2019.

[28] P. Ladosz, H. Oh, W. Chen, Optimal Positioning of Communication Relay Unmanned Aerial Vehicles in Urban Environments, *2016 International Conference on Unmanned Aircraft Systems (ICUAS)*, Arlington, VA, 2016, pp. 1140-1147.

[29] Y. Chen, N. Zhao, Z. Ding, M. Alouini, Multiple UAVs as Relays: Multi-hop Single Link versus Multiple Dual-hop Links, *IEEE Transactions on Wireless Communications*, Vol. 17, No. 9, pp. 6348-6359, September, 2018.

[30] J. Cortes, Discontinuous Dynamical Systems, *IEEE Control Systems Magazine*, Vol. 28, No. 3, pp. 36-73, June, 2008.

[31] R. C. M. Brekelmans, L. T. Driessen, H. J. M. Hamers, D. den. Hertog, Gradient Estimation Schemes for Noisy Functions, *Journal of Optimization Theory and Applications*, Vol. 126, No. 3, pp. 529-551, September, 2005.

[32] M. Barros, M. Casquilho, Linear Programming with CPLEX: An Illustrative Application over the Internet CPLEX in

Fortran 90, *2019 14th Iberian Conference on Information Systems and Technologies (CISTI)*, Coimbra, Portugal, 2019, pp. 1-6.

Biographies

Tao Peng received the B.S., M.S. and Ph.D. degrees from Beijing University of Posts and Telecommunications (BUPT), Beijing, China, in 1999, 2002 and 2010 respectively. He is now associate Professor at the School of Information and Communications Engineering, BUPT. His current research interests include AI-based communications and networks, MANET, etc.

Xiaoyang Li received the B.S. degrees from Beijing University of Posts and Telecommunications (BUPT), Beijing, China, in 2018. He is currently studying for a master's degree in BUPT. During the graduate period, he is mainly engaged in the research of drone communication.

Xiangyu Li received the B.S. degrees from China University of Petroleum (UPC), Shandong, China, in 2017 and M.S. degrees from Beijing University of Posts and Telecommunications (BUPT), Beijing, China, in 2020. Research in the field of drone communication during postgraduate period.

Rongrong Qian received the B.S. degree in communication engineering from Beijing Univ. of Posts and Telecomm.(BUPT), Beijing, China, and the Ph.D. degree in signal and information processing from BUPT, in 2004 and 2010, respectively. His is now an Associate Professor with the School of Artificial Intelligence, BUPT.